High-Resolution, Nonhydrostatic Simulations of Internal Wave Generation in the Luzon Strait using SUNTANS

Oliver B. Fringer
473 Via Ortega, Room 187
Dept. of Civil and Environmental Engineering
Stanford University
Stanford, CA 94305
phone: (650) 725-6878 fax: (650) 725-9720 email: fringer@stanford.edu

LONG-TERM GOALS

The long term goal is to develop the capability to predict the internal wave climate in the ocean with the high-resolution, three-dimensional, nonhydrostratic SUNTANS model.

OBJECTIVES

Our primary objective is to understand the mechanisms leading to the generation of internal waves in the South China Sea by performing high-resolution, nonhydrostatic numerical simulations with the SUNTANS model. A secondary objective is to perform simulations to aid with the planning of the field experiments for the IWISE (Internal Waves in Straits Experiment) DRI.

APPROACH

We are employing a combination of theoretical analyses and numerical simulations with the SUNTANS (Fringer et al., 2006) model to perform a detailed, nonhydrostatic study of the mechanisms governing the generation of internal waves in the Luzon Strait, which forms the eastern boundary of the South China Sea (see Figure 1). Our work builds upon simulations we have performed as part of the NLIWI (Nonlinear Wave Initiative) DRI that have been designed to understand the generation and propagation of internal waves in the South China Sea, as well as how the internal waves interact with the continental shelf on the western side of the sea. The simulations are similar to the NLIWI simulations but focus on the Luzon Strait. We plan on performing simulations in smaller-scale domains in order to focus on the generation region, rather than full basin-scale domains, which are better-suited to studying internal wave generation and the deep-basin propagation and interaction with the Dongsha Plateau and the Chinese continental shelf (see Figure 1). SUNTANS domains for the present work are targeted towards simulating high-resolution, nonhydrostatic flow physics through channels and over sills to understand the fundamental physics of internal wave generation. We expect the grid to be refined around the Babuyan and Batan Islands in order to highly resolve the tidal flow around these islands and to resolve possible hydraulic control features. Based on our experience with

1

Report Documentation Page		*Form Approved* *OMB No. 0704-0188*

Public reporting burden for the collection of information is estimated to average 1 hour per response, including the time for reviewing instructions, searching existing data sources, gathering and maintaining the data needed, and completing and reviewing the collection of information. Send comments regarding this burden estimate or any other aspect of this collection of information, including suggestions for reducing this burden, to Washington Headquarters Services, Directorate for Information Operations and Reports, 1215 Jefferson Davis Highway, Suite 1204, Arlington VA 22202-4302. Respondents should be aware that notwithstanding any other provision of law, no person shall be subject to a penalty for failing to comply with a collection of information if it does not display a currently valid OMB control number.

1. REPORT DATE **2009**	2. REPORT TYPE	3. DATES COVERED **00-00-2009 to 00-00-2009**

4. TITLE AND SUBTITLE **High-Resolution, Nonhydrostatic Simulations of Internal Wave Generation in the Luzon Strait using SUNTANS**	5a. CONTRACT NUMBER
	5b. GRANT NUMBER
	5c. PROGRAM ELEMENT NUMBER
6. AUTHOR(S)	5d. PROJECT NUMBER
	5e. TASK NUMBER
	5f. WORK UNIT NUMBER

7. PERFORMING ORGANIZATION NAME(S) AND ADDRESS(ES) **Stanford University,Dept. of Civil and Environmental Engineering,473 Via Ortega, Room 187,Stanford,CA,94305**	8. PERFORMING ORGANIZATION REPORT NUMBER

9. SPONSORING/MONITORING AGENCY NAME(S) AND ADDRESS(ES)	10. SPONSOR/MONITOR'S ACRONYM(S)
	11. SPONSOR/MONITOR'S REPORT NUMBER(S)

12. DISTRIBUTION/AVAILABILITY STATEMENT
Approved for public release; distribution unlimited

13. SUPPLEMENTARY NOTES

14. ABSTRACT

15. SUBJECT TERMS

16. SECURITY CLASSIFICATION OF:			17. LIMITATION OF ABSTRACT	18. NUMBER OF PAGES	19a. NAME OF RESPONSIBLE PERSON
a. REPORT **unclassified**	b. ABSTRACT **unclassified**	c. THIS PAGE **unclassified**	**Same as Report (SAR)**	**7**	

Standard Form 298 (Rev. 8-98)
Prescribed by ANSI Std Z39-18

simulating internal waves in the SCS, we expect to be able to use SUNTANS in a predictive manner to aid in the placement of instrumentation for the field component of the IWISE DRI.
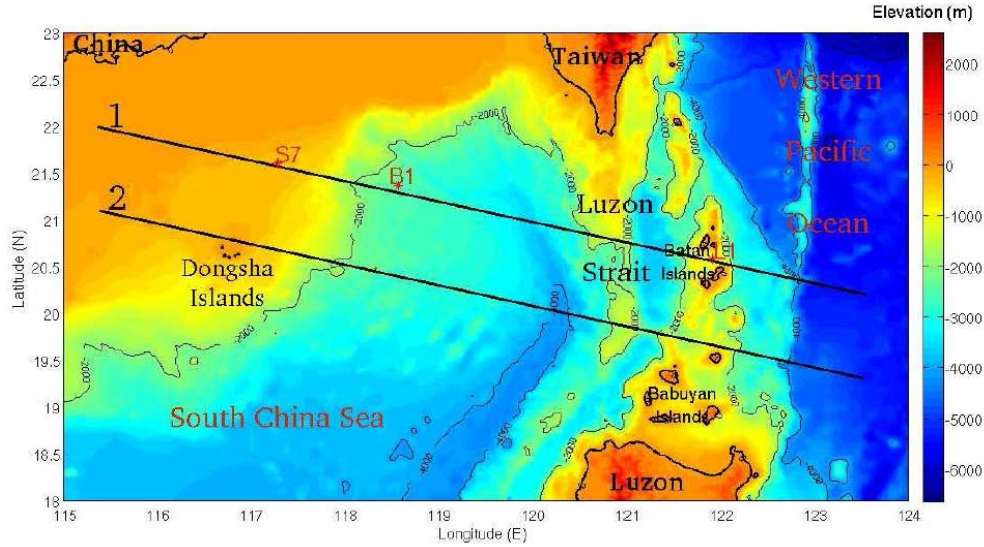

Figure 1: Bathymetric map of the South China Sea, showing the locations of mooring sites L1, B1 and S7 from the WISE/VANS project in 2005, and the transects that are used for the two-dimensional theoretical analysis.

WORK COMPLETED

We have developed a linear theory for the generation of internal waves over ridges to determine the phase in the tide at which peaks in the depression waves cross the ridges.

RESULTS

The most basic aspect of nonlinear internal waves in the South China Sea that has yet to be explained is the correlation of peaks in westward-propagating internal waves with maximum eastward (ebb) currents at the eastern ridge in the Luzon Strait. Ramp et al. (2004) used linear theory to compute the internal wave phase speeds and trace peaks in the internal wave signatures observed at B1 back to mooring L1, and showed that the tracebacks always crossed mooring L1 during peak eastward tidal flow. The lee-wave release mechanism proposed by Maxworthy (1979) is a plausible generation mechanism because it implies that a hydraulic control develops over the ridge at L1 that prevents waves from propagating westward until the tide becomes subcritical. This mechanism is unlikely because waves appear to be "released" during peak easward tidal flow at the ridge throughout the spring-neap cycle during which time the peak ebb currents range from strongly supercritical to subcritical, and the lee-wave mechanism is not possible unless the tidal currents are supercritical. Zhao and Alford (2006) proposed an alternate mechanism in which waves are generated over the eastern ridge during peak flood tidal currents (westward), and these waves steepen into trains of nonlinear waves as they propagate into the basin. Although they proposed a different mechanism, Zhao and Alford (2006) also found that the generation phase was independent of the strength of the tidal currents.

2

The theoretical analysis that we have developed is based on the hypothesis that the generation mechanism is dominated by linear processes, and this is based on the evidence that wave arrival time at a particular mooring in the basin is roughly the same relative to the phase in the particular tide that generated that wave. That is, diurnally-generated A-waves (Ramp et al. 2004) arrive at mooring S7 at the same time every day, while semidiurnally-generated B-waves (Ramp et al. 2004) arrive roughly one hour later each day. This implies that hydraulic effects at the generation site are weak and that nonlinear effects on the propagation speed are also weak. These justify development of a linear model, which is further simplified by assuming that the internal tides are generated and propagate predominantly as first-mode waves, which is based on evidence, both from modeling and observations, that more than 90% of the internal tidal energy in the Luzon Strait is in the first mode (Simmons 2009).

The linear model is derived from the inviscid equations of motion with the Boussinesq approximation for a two-layer fluid with upper-layer depth d_1 and lower-layer depth d_2, with the free-surface defined by η and the interface between the layers defined by ζ, and with the bottom bathymetry defined by h, as shown in Figure 2.
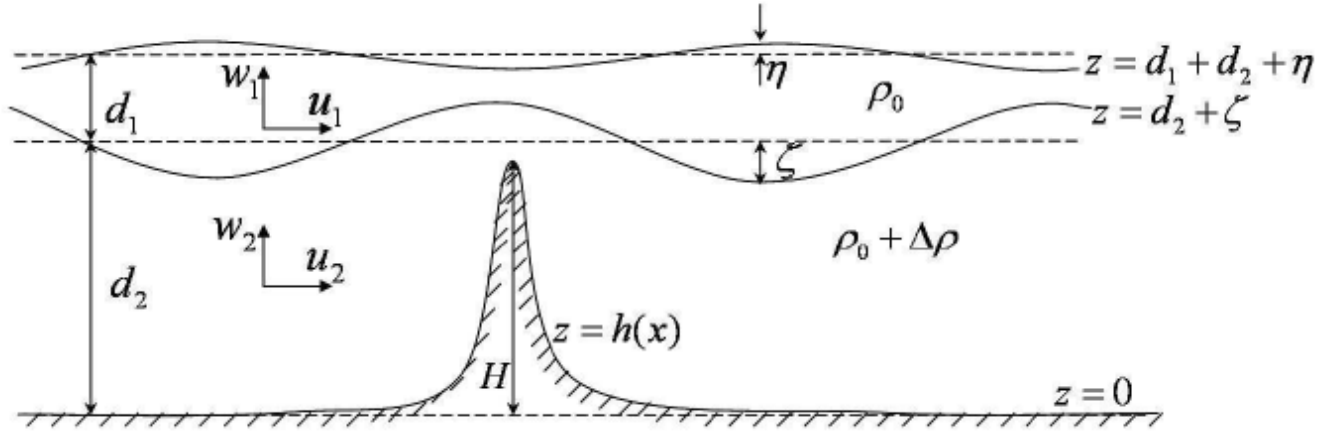

Figure 2: Schematic of the two-layer system used to develop the linearized equations.

The equations of motion for the velocities in the upper layer, u_1, v_1, and lower layer, u_2, v_2, along with continuity, are given by

$$\frac{\partial \eta}{\partial t} = -\frac{\partial}{\partial x}\left[u_1\left(d_1 + \eta - \zeta\right)\right] - \frac{\partial}{\partial x}\left[u_2\left(d_2 + \zeta - h\right)\right],$$

$$\frac{\partial \zeta}{\partial t} = -\frac{\partial}{\partial x}\left[u_2\left(d_2 + \zeta - h\right)\right],$$

$$\frac{\partial u_1}{\partial t} + u_1\frac{\partial u_1}{\partial x} - fv_1 = -g\frac{\partial \eta}{\partial x},$$

$$\frac{\partial u_2}{\partial t} + u_2\frac{\partial u_2}{\partial x} - fv_2 = -g\frac{\partial \eta}{\partial x} - g'\frac{\partial \zeta}{\partial x},$$

$$\frac{\partial v_1}{\partial t} + fu_1 = 0,$$

$$\frac{\partial v_2}{\partial t} + fu_2 = 0,$$

where f is the Coriolis parameter and we have assumed quasi two-dimensionality by ignored all gradients of v and all gradients with respect to y. After linearization and assuming a rigid lid, weak topography ($\alpha = h/d_2 <<1$) and a shallow upper layer ($\beta = d_1/d_2 <<1$), the nondimensional equation govering the behavior of the interface when subjected to a half-cosined-shaped ridge is given by the inhomogeneous Klein-Gordon equation,

$$\zeta_{tt} + \frac{1}{R^2}\zeta - \frac{1}{1+\beta}\zeta_{xx} = -Af(x)\sin(k_b x)\cos(t),$$

where $R = \omega/f$ is the Rossby number and ω is the tidal frequency, k_b is the nondimensional wavenumber of the topography. Here, x is the nondimensional distance and t is the nondimensional time, such that, if * represents a dimensional quantitity, then $x=kx^*$ and $t=\omega t^*$, and $k=2\pi/\lambda$ is the internal tidal wavenumber and λ is its wavelength, for $\beta=0$ and $R=\infty$. In the governing equation for z, $f(x) = H(x - \pi/k_b)H(-x + \pi/k_b)$ and $H(x)$ is the heaviside function, and the amplitude is given by

$$A = \frac{1}{2}\alpha\beta k_b F_0\left(1 - \frac{1}{R^2}\right),$$

where in the present analysis $F_0=1$. The solution for ζ is given by a standing wave in the region $|x|<\pi/k_b$,

$$\zeta_C = -\frac{\zeta_0}{2\sin(k_0\pi/k_b)}\left[\frac{2k_0}{k_b}\sin(k_b x)\cos(t) + \sin\left(k_0 x + t - \frac{k_0\pi}{k_b}\right) + \sin\left(k_0 x - t + \frac{k_0\pi}{k_b}\right)\right]$$

and freely-propagating waves that radiate away to the left and right of the ridge (located at $x=0$),

$$\zeta_L = \zeta_0\cos(k_0 x + t) \quad (x < -\pi/k_b),$$

$$\zeta_R = -\zeta_0\cos(k_0 x - t) \quad (x > \pi/k_b),$$

where the amplitude of the waves that radiate away is given by

$$\zeta_0 = \frac{1}{2}\alpha k_b F_0 \frac{\beta}{(1+\beta)^2} G(k_0/k_b) \, ,$$

and the function G is given by

$$G(\gamma) = \frac{\gamma \sin(\pi\gamma)}{1 - \gamma^2} \quad .$$

The nondimensional wavenumber of the waves in the presence of rotation is given by the dispersion relation for Poincare waves

$$c_i^2 k_0^2 = 1 - \frac{1}{R^2} \, .$$

where $c_i^2 = (1+\beta)^{-1}$. This solution shows that the phase in the tide in which troughs in left- or westward-propagating linear waves cross the sill is strong function of k_0/k_b, since the function G is not monotonic. For most problems of interest, k_0/k_b is small since the scale of the topography is typically of the order of or smaller than the internal tidal wavelength. However, different values can lead to wave generation at different tidal phases. Figure 3 depicts the analytical result for four different values of k_0/k_b, and shows that for $k_0/k_b=0.5$, *1.5, and 3.5* (Figures 3(a), (b) and (d)), left-propagating depressions coincide with the end of the ebb (eastward) tide, while for $k_0/k_b=2.5$ (Figure 3(c)), left-propagating waves coincide with the end of the flood (westward) tide. Therefore, because the value of k_0/k_b affects the sign of G, the ratio of the topographic scale to the wavelength of the internal tide determines the apparent phase in the tide at which depressions are generated. Short topography relative to the internal tidal wavelength yields westward-propagating waves that originate at the end of the ebb tide, while longer waves can alternate between the end of the ebb and the end of the flood tide.

These results are contrary to the observations because they indicate that waves are generated during slack rather than peak tides. We hypothesize that the linear theory will show that a two-ridge system can lead to left-propagating waves that are generated during peak ebb tides over the eastern ridge, and that nonlinear effects are not significant in altering this behavior. This is the subject of ongoing work.
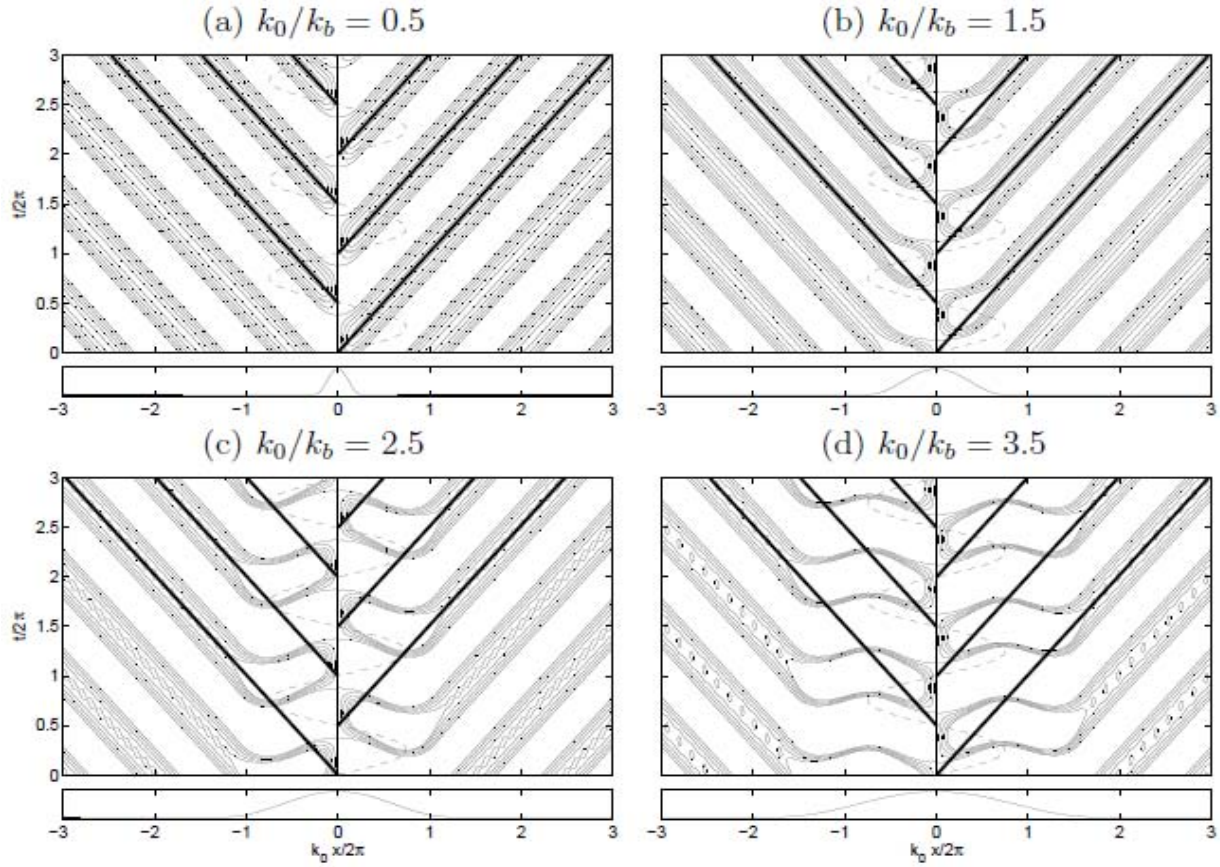
Figure 3: Contours of ζ= −(0, 0.25, 0.5, 0.75, 0.95)ζ₀ depicting the influence of the relative width of the sill on the trajectories of depresssion waves that emerge over the course of three tidal cycles. The dashed line indicates the direction and relative magnitude of the barotropic currents while the dark solid lines trace out the peak depressions as they propagate to the left and right of the sill. The small plots indicate the shape of the bathymetry for reference.

IMPACT/APPLICATIONS

Understanding internal tides and waves is important for developing parameterizations of their effects in larger-scale ocean models.

REFERENCES

Fringer, O. B., Gerritsen, M., and R. L. Street, 2006, An unstructured-grid, finite-volume, nonhydrostatic, parallel coastal ocean simulator, Ocean Modelling, 14 (3-4), 139-278, doi:10.1016/J.OCEMOD.2006.03.006.

Maxworthy, T. (1979), A note on the internal solitary waves produced by tidal flow over a three-dimensional ridge, J. Geophys. Res., 84, 338-346.

Ramp, S. R., Tang, T. Y., Duda, T. F., Lynch, J. F., Liu, A. K., Chiu, C.-S., Bahr, F., Kim, H.-R., and Y. J. Yang, 2004, Internal solitons in the northeastern South China Sea part I: Sources and deep water propagation, IEEE J. Oceanic Eng., 29, 1157-1181.

Zhao, Z., and M. H. Alford (2006), Source and propagation of internal solitary waves in the northeastern South China Sea, J. Geophys. Res., 111, C11012, doi:10.1029/2006JC003644.

PUBLICATIONS

Fringer, O. B., 2009, Multiscale numerical simulation of internal waves in the ocean, The 4th Warnemünde Turbulence Days (WTD) on Internal Waves and Turbulence in Coastal Seas (invited).

HONORS/AWARDS/PRIZES

Oliver B. Fringer, Presidential Early Career Award, 2009.